IET Optoelectronics

Research Article

IET Journals
The Institution of Engineering and Technology

Semiconductor optical amplifiers for underwater optical wireless communications

ISSN 1751-8768
Received on 21st January 2016
Revised 3rd June 2016
Accepted on 10th July 2016
doi: 10.1049/iet-opt.2016.0010
www.ietdl.org

Kostas P. Peppas[1] ✉, Anthony C. Boucouvalas[1,2], Zabih Ghassemloy[2], Mohhamad-Ali Khalighi[3], Kostas Yiannopoulos[1], Nikos C. Sagias[1]

[1]*Department of Informatics and Telecommunications, University of Peloponnese, Tripoli 22131, Greece*
[2]*Faculty of Engineering and Environment, University of Nothumbria, Ellison Building, Newcastle, UK*
[3]*Institut Fresnel, Ecole Centrale Marseille, Marseille, France*
✉ *E-mail: peppas@uop.gr*

Abstract: Underwater optical wireless communications (UOWC) systems have recently received significant attention as an attractive solution for both research and commercial use because of their ability to provide high bandwidth communications over relatively short transmission spans along with their low operational cost. However, high absorption and scattering of optical transmission in the water limit the achievable range of underwater optical wireless links to only few metres. In this study, in an effort to increase the range and reliability of underwater optical wireless links, the authors propose to utilise semiconductor optical amplifiers at the receiver and discuss in a quantitative fashion the performance enhancements that can be achieved. After developing the required analytical framework, extensive numerical results are further provided to demonstrate the performance of the proposed scheme for different operating conditions. Specifically, assuming intensity modulation and direct detection schemes with on–off keying modulation, they evaluate the bit error rate of the proposed system configuration for different water types, link distances and forward error correction schemes. Performance evaluation results reveal that the use of optical amplification can significantly improve the quality of UWOC links.

1 Introduction

Underwater optical wireless communication systems (UOWC) are rapidly gaining popularity as cost-effective means of transferring data at high rates over short ranges [1]. UOWC systems, usually operating in the blue/green spectrum region where absorption is minimum compared with other wavelengths, are regarded as an attractive candidate technology to provide secure, efficient and high data rate communications among submarines, unmanned underwater vehicles, ships, divers, buoys and underwater sensors within short range.

However, UOWC links suffer from the absorption and the spatial dispersion of photons due to scattering along the transmission path. Natural oceans are rich in dissolved and particulate matter, leading to a large range of conditions that an underwater communication system must satisfy. Also, seawater strongly scatters light, thus reducing the photon density at the receiver and severely degrading the bit error rate (BER) performance of UOWC links, especially in turbid harbour and coastal waters [2–4].

UOWC systems have been addressed in several research works including [5–7] and references therein. For example in [5], the performance of a UOWC network consisting of uniformly distributed nodes is assessed. In [6], vector radiative transfer theory is employed to provide a realistic model of the UOWC channel. In [7], different configurations of UOWC networks with line-of-sight and non-line-of-sight links were investigated. In all the above mentioned research works, high absorption and scattering of optical transmission in the water, limits the use of UOWC systems to only few metres. Therefore, efficient schemes should be utilised to compensate for the detrimental impact of such propagation mechanisms and improve the quality of UWOC links.

Motivated by the need to develop high data rate and error-free UOWC systems, in this paper we propose to employ semiconductor optical amplifiers (SOA) at the receiver. SOA amplification has been recently proposed as an attractive approach for atmospheric turbulence compensation in free-space optical communication links [8–10]. Further justification for the employment of SOA amplification comes from the fact that the optical amplifier can significantly improve receiver sensitivity [11, 12]. To the best of the authors' knowledge, however, optical amplification has not so far been applied to UOWC links and thus is the topic of our contribution. Moreover, for UOWC links it is still not clear to what extent SOA amplification can enhance system performance.

It should be noted, however, that the operational wavelength of current SOA amplifiers ranges from 850 to 1600 nm. Nevertheless, in a recent work [13], it was shown that a small-signal gain of 19 dB is achievable with a very compact optical amplifier with a 400 μm wavelength. Moreover, in [14] the basic characteristics of GaN-based SOAs were reviewed, focusing on pulse amplification. GaN-based SOAs can potentially cover a particularly wide spectral range, from the deep ultra violet to the infrared and can be employed in a variety of applications that utilise short wavelength, ultra-fast pulses. Since UOWC systems are more efficient at blue–green frequencies, one can envisage the use of such devices to provide significant performance enhancements.

System performance is quantified by the BER assuming both uncoded and coded UOWC systems. Extensive numerical results are presented to demonstrate the proposed analysis. The remainder of this paper is structured as follows: Section 2 outlines the system and channel models. In Section 3, an analytical expression for the BER performance of the proposed system is deduced. Numerical results are provided in Section 4 while Section 5 concludes the paper with a summary of the main results.

2 Channel and system models

2.1 UOWC model

Photon transport in an underwater propagation medium can be modelled analytically by the so-called radiative transfer equation (RTE) as [15, (4)]

$$\frac{\mathrm{d}L}{\mathrm{d}r} = -cL + L^{\mathrm{E}} + L^{\mathrm{I}}. \quad (1)$$

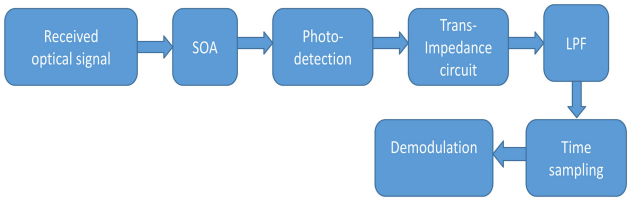

Fig. 1 *Block diagram of the receiver*

In (1), $L(r,\theta,\phi,\lambda)$ is the optical radiance at position (r, θ, ϕ) with unit of $\mathrm{Wm^{-2}\,sr^{-1}\,nm^{-1}}$, where r is the distance from the transmitter and θ and ϕ are the polar and azimuthal angles, respectively. Furthermore, $c(\lambda)$ is the attenuation coefficient of the aquatic medium which depends on wavelength λ and on water type and L^{E}, L^{I} are functions related to elastic and inelastic scattering, respectively. It is noted that the RTE is an integro-differential equation of several independent variables and, in general, an analytical solution is difficult to be obtained. In this work, instead of solving (1) analytically, we turned our attention to [15] in which a Monte Carlo-based approach is used to solve the RTE. We then carefully extracted simulation points from Fig. 4 of [15] and henceforth evaluated optical radiance for different water types and link distances.

2.2 System model

Consider an UOWC system as shown in Fig. 1. The received optical signal traverses the corresponding SOA and receive a static gain equal to G. The amplified signal is then focused onto a photo-detector (PD), which converts the received optical field to an electrical signal. A transimpedance circuit amplifies the resulting photo-current and converts it to a voltage. The electrical signal passes through a low pass filter, is time sampled and finally demodulated to retrieve the resulting bits. In what follows, it is assumed that the saturation of the optical amplifier is negligible and that a small signal gain is always obtained.

At the SOA output, an additional optical noise component due to amplified spontaneous emission is also generated. The spectral density of this component is given by [16, 17]

$$P_n = \frac{n_{\mathrm{sp}}\mathrm{h}c}{\lambda} \tag{2}$$

where c denotes the speed of light in vacuum, $h = 6.6 \times 10^{-34}$ Js is Planck's constant and n_{sp} is the population inversion factor. Shot noise is also present with variance equal to [8]

$$\sigma^2_{\mathrm{shot}}(P_{\mathrm{in}}) = 2q_{\mathrm{e}}R\big(GP_{\mathrm{in}} + (G-1)P_nB_0\big)B_{\mathrm{e}} \tag{3}$$

where P_{in} is the power at the input of the SOA, $q_{\mathrm{e}} = 1.6 \times 10^{-19}$ C is the charge of an electron, R is the photodiode responsivity and B_{e} and B_0 are the electrical and optical bandwidths, respectively. In addition, thermal noise is also added to the received signal and its variance is deduced as

$$\sigma^2_{\mathrm{th}} = \frac{4k_{\mathrm{B}}TF_{\mathrm{n}}B_{\mathrm{e}}}{R_{\mathrm{L}}} \tag{4}$$

where $k_{\mathrm{B}} = 1.38 \times 10^{-23}\mathrm{J/K}$ is the Boltzmann's constant, T is the receiver temperature in Kelvin, F_{n} is the electric noise figure and R_{L} is the load resistance of the PD. Finally, signal-spontaneous beating and spontaneous–spontaneous beating noise components are present and their variances are expressed as [8]

$$\sigma^2_{\mathrm{sig-sp}}(P_{\mathrm{in}}) = 4R^2GP_{\mathrm{in}}(G-1)P_nB_{\mathrm{e}} \tag{5a}$$

$$\sigma^2_{\mathrm{sp-sp}} = R^2\big((G-1)P_n\big)^2(2B_0 - B_{\mathrm{e}})B_{\mathrm{e}} \tag{5b}$$

3 Performance analysis

Hereafter we consider intensity modulation and direct detection schemes with on–off keying (OOK) modulation, where the required bandwidth B_{e} is equal to the transmission rate R_{b}. Assuming that the symbol '1' was transmitted, the signal and noise powers can be deduced as

$$I_1 = RP_{\mathrm{out}} \tag{6a}$$

$$\sigma^2_1 = \sigma^2_{\mathrm{th}} + \sigma^2_{\mathrm{shot}} + \sigma^2_{\mathrm{sig-sp}} + \sigma^2_{\mathrm{sp-sp}}. \tag{6b}$$

The corresponding signal and noise powers when the symbol '0' was transmitted can be expressed as

$$I_0 = 0 \tag{7a}$$

$$\sigma^2_0 = \sigma^2_{\mathrm{th}} + \sigma^2_{\mathrm{shot}}(0) + \sigma^2_{\mathrm{sp-sp}} \tag{7b}$$

In what follows, it is assumed that perfect channel state information is available at the receiver side. Thus, the receiver can set the decision threshold as [18]

$$I_{\mathrm{th}} = \frac{\sigma_0 I_1}{\sigma_0 + \sigma_1}. \tag{8}$$

On the basis of the above analysis, the probability of a bit error, P_{b}, of an uncoded UOWC system is deduced as

$$P_{\mathrm{b}} = \frac{1}{2}\mathrm{erfc}\left[\frac{I_1}{\sqrt{2}(\sigma_0 + \sigma_1)}\right]. \tag{9}$$

Next, a (n,k) Reed–Solomon (RS) error correction code with a q-bit symbol alphabet GF(K) is considered, where $n = K - 1$ and $K = 2^q$. This code can correct up to $t = (n-k)/2$ symbol errors. The theoretical error-correction capability of the considered RS code is characterised by the following upper bound [19]:

$$P_{\mathrm{us}} = \frac{1}{n}\sum_{i=t+1}^{n} i\binom{n}{i}P_{\mathrm{b}}^i(1-P_{\mathrm{b}})^{n-i} \tag{10}$$

where P_{us} is the probability of uncorrectable symbol error and P_{b} is readily obtained from (9).

4 Numerical results and discussion

In this section, a set of analytical results is presented to demonstrate the potential performance enhancements obtained by the incorporation of SOA amplifiers. The model parameters are presented in Table 1.

The system under consideration is assumed to be deployed in deep-sea waters. Thus, no spatial filtering is considered at the receiver, because background radiations can be effectively neglected. Two water types are considered, namely clean ocean and coastal waters, having attenuation coefficient $c(\lambda)$ equal to 0.15 and 0.305, respectively. It is also assumed that the system under consideration employs wide pulses and thus pulse broadening due to the aquatic channel can be neglected. According to the default parameters presented in [15, Table 2], pulse broadening is <0.3 ns. Thus, since a data rate of 100 Mbps is considered, inter-symbol interference (ISI) can be ignored for the considered water types. It should also be pointed out that, based on [15], the impact of ISI is practically an issue for high turbidity waters only.

For the purposes for this work we assume direct coupling and large coupling efficiency, i.e. 100%. With respect to the amplifier input and output coupling efficiencies, they were also considered to be ideal (100%) so as to limit the number of parameters under consideration for the amplifier model. A treatment that also takes into account non-ideal amplifier couplings is feasible by modifying (3), (5) and (6b) following the analysis presented in [11]. A line-of-sight configuration is considered and perfect alignment between the transmitter and the receiver is assumed [15]. A lens of diameter

D of 20 cm is used at the receiver side and a high speed PD is placed on its focal point.

As a practical example, we consider an Si-PIN PD having a responsivity of $R(\lambda) = 0.35\,\text{A/W}$ at $\lambda = 532\,\text{nm}$. These parameters correspond to a *Hamamatsu S10784* PIN PD-based receiver [21]. A beam width of 3 mm and a maximum transmitter beam divergence of 20° is also assumed. The normalised received power on the PD active area was obtained by extracted simulation points from Fig. 4 of [15], assuming that photon angle scattering is modelled by the so-called two-term Henyey–Greenstein model [22]. Tables 2 and 3 present values for the normalised received intensity in dB for various link distances, r, assuming clear ocean and coastal waters, respectively.

Fig. 2 illustrates the BER performance of SOA- and non-SOA-assisted receivers against the transmit power P_t for the uncoded case assuming a propagation distance r of 15 or 20 m, SOA gain of 10 dB and clear ocean waters. As it is evident, the average BER significantly improves when SOA amplification is employed. Moreover, when optical amplification is employed, the system under consideration yields sufficient performance for r of 15 m and P_t of ∼−7 dBm, as well as for r of 20 m and P_t of ∼−2.2 dBm at a target BER of 10^{-9}.

Table 1 Simulation parameters [7–9, 15, 20]

Parameter	Value
wavelength, λ	532 nm
data rate, R_b	100 Mbps
optical bandwidth, B_0	50 GHz
attenuation coefficient, $c(\lambda)$	0.15, 0.305 m^{-1}
SOA small-signal gain, G	10, 15 or 20 dB
population inversion factor, n_{sp}	4.0
detector responsivity, $R(\lambda)$	0.35 A/W
resistor load, R_L	100 Ω
electrical noise figure, F_n	3 dB
receiver temperature, T	256 K
receiver lens diameter, D	20 cm
beam width	3 mm
maximum transmitter beam divergence	20°

Table 2 Normalised received intensity in dB as a function of link distance, r, for clear ocean, based on [15, Fig. (4)]

Link distance, m	Received intensity, dB
5.4	−12.138
10.5	−18.896
15.1	−25.379
20.2	−30.069
25.1	−34.345
30.1	−38.344
35.0	−42.207
39.9	−45.931
44.9	−49.931
49.9	−53.655
54.8	−56.965
59.7	−60.827
64.6	−64.138
69.7	−67.724

Table 3 Normalised received intensity in dB as a function of link distance, r, for coastal waters, based on [15, Fig. (4)]

Link distance, m	Received intensity, dB
5.3	−14.069
10.3	−22.896
15.2	−32.276
20.1	−39.448
25.1	−46.621
30.2	−54.345
35.1	−60.689

Fig. 3 depicts the error performance of SOA- and non-SOA-assisted receivers against P_t for the uncoded case assuming a propagation distance of 10 or 15 m, SOA gain of 10 dB and coastal waters. As it can be observed, when optical amplification is employed, the considered system can achieve a BER of 10^{-9} for r of 10 m and P_t of ∼−9.5 dBm. Nevertheless, BER significantly deteriorates as r increases from 10 to 15 m. Specifically, in this case, a BER of 10^{-9} can be achieved for P_t of ∼0 dBm.

Figs. 4 and 5 depict the error performance of SOA-assisted receivers as a function of r for P_t of 0 dBm, and a range of SOA gains, $G = \{10, 15, 20\}$, for clear ocean and coastal water, respectively. It is evident that link distance significantly increases as G increases, depending on the water type. Specifically, a BER of 10^{-9} can be achieved at distances of ∼23, 28 and 32.5 m for clear ocean and SOA gain of 10, 15 and 20, respectively. For coastal water, the corresponding distances are ∼15, 19.5 and 21 m for SOA gain of 10, 15 and 20, respectively.

Figs. 6 and 7 depict the error performance of SOA-assisted receivers when forward error correction is employed as a function of P_t for SOA gain G of 20 and for clear ocean and coastal water, respectively. The propagation distance r is equal to 30 and 20 m for clear ocean and coastal water, respectively. The coding schemes under consideration are the RS(255,239), RS(255,223) and RS(255,207) [19]. These RS codes can, respectively, correct up to 8, 16 and 24 symbol errors, each symbol having a length of 8 bits. As it can be observed, forward error correction can achieve an error probability of 10^{-9} for values of P_t between ∼−7 and −5.5 dBm for clear ocean and r of 30 m as well as for values of P_t between ∼−6 and −4.4 dBm for coastal water and r of 20 m. Finally, in Fig. 8 we consider an SOA-assisted UOWC system operating in coastal water and employing forward error correction. The propagation distance r is equal to 35 m, the SOA gain G is equal to 20 and the transmit power, P_t, ranges from 0 to 20 dBm. As it can be observed, for the specific system configuration the RS(255,207) can achieve an error probability of 10^{-9} for P_t between ∼15.2 and 17 dBm. It can be observed that the uncoded system cannot accommodate the required performance criterion for the considered system configuration.

5 Conclusions

In this work, we proposed to employ SOA amplification as an efficient means to improve the reliability of underwater optical wireless links. For the system under consideration, we derived BER expressions for uncoded and coded UOWC links with OOK. Our results demonstrated that the use of SOA amplification at the receiver can significantly enhance the quality of UOWC systems, similar to Free Space Optical ones. In comparison to the conventional UOWC system without amplification, it was shown that the SOA-assisted system can increase the propagation distance. Finally, our newly derived analytical results can serve as a simple yet reliable method to estimate BER performance of SOA-assisted UOWC links.

6 Acknowledgment

The authors acknowledge support by the COST Action IC1101 OPTICWISE (Optical Wireless Communications – An Emerging Technology).

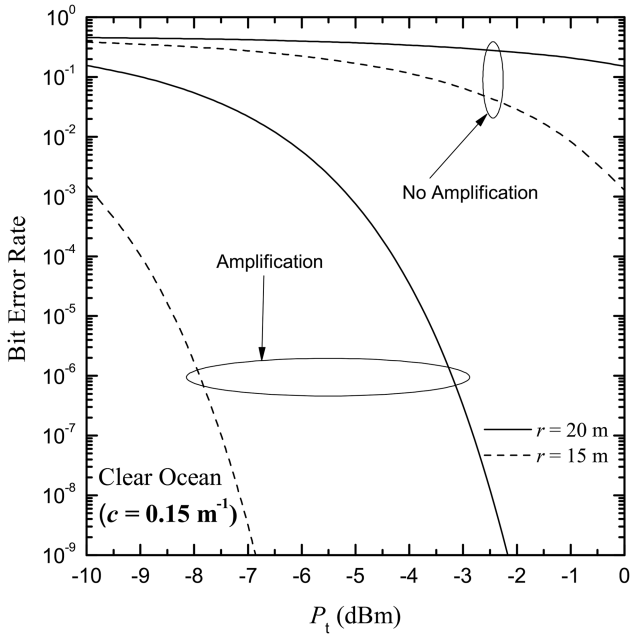

Fig. 2 *BER of uncoded SOA- and non-SOA-assisted systems as a function of P_t assuming clear ocean (c = 0.15 m^{-1}), SOA gain G of 10 dB and link distances of 15 or 20 m*

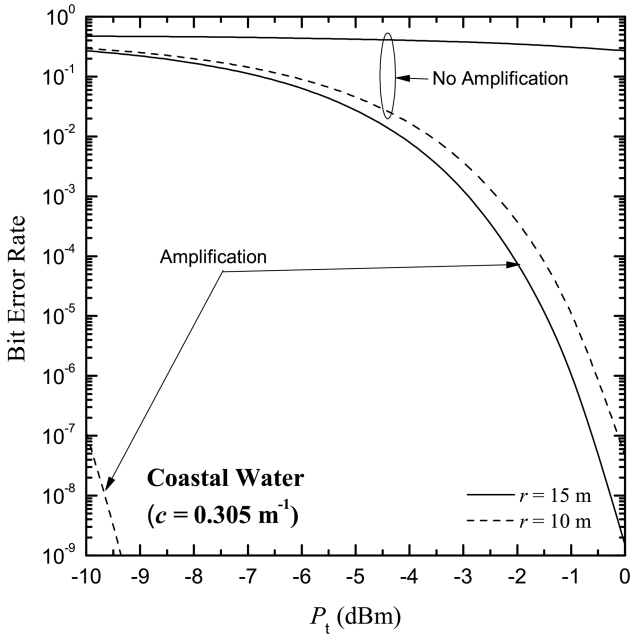

Fig. 3 *BER of uncoded SOA- and non-SOA-assisted systems as a function of P_t assuming coastal water, (c = 0.305 m^{-1}), SOA gain G of 10 dB and link distances of 15 or 20 m*

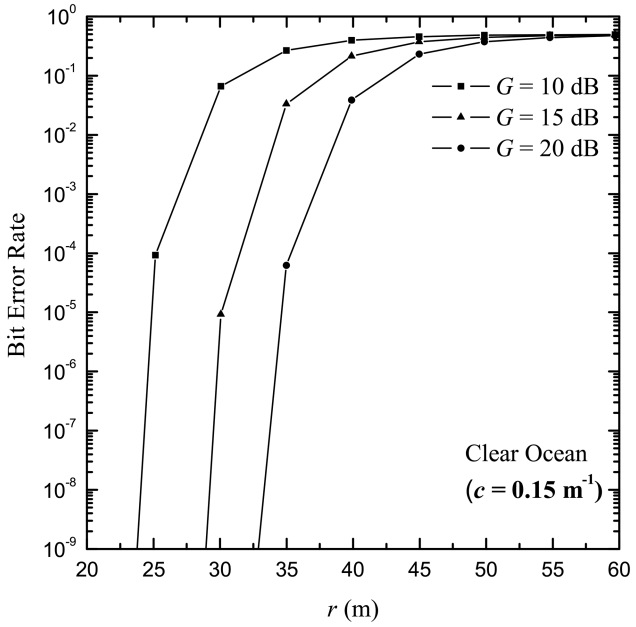

Fig. 4 *BER of uncoded SOA-assisted systems as a function of link distance, r assuming clear ocean (c = 0.15 m^{-1}), for a range of SOA gains G and transmit power of 0 dBm*

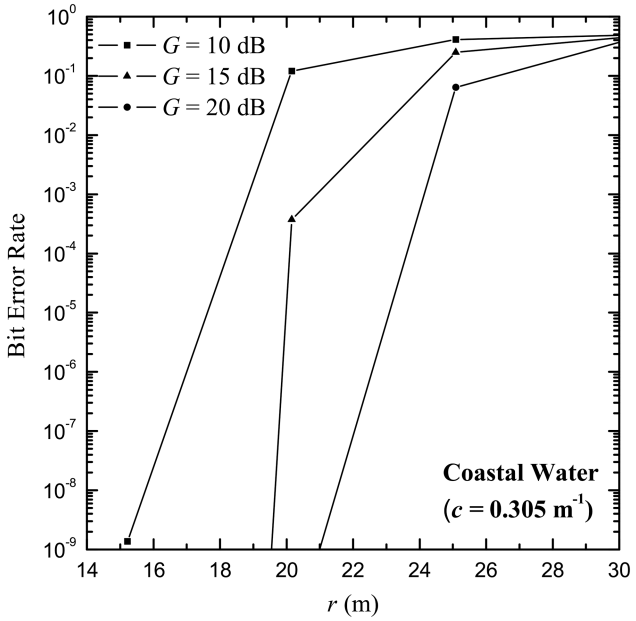

Fig. 5 *BER of uncoded SOA-assisted systems as a function of link distance, r assuming coastal water (c = 0.305 m^{-1}), for a range of SOA gains G and transmit power of 0 dBm*

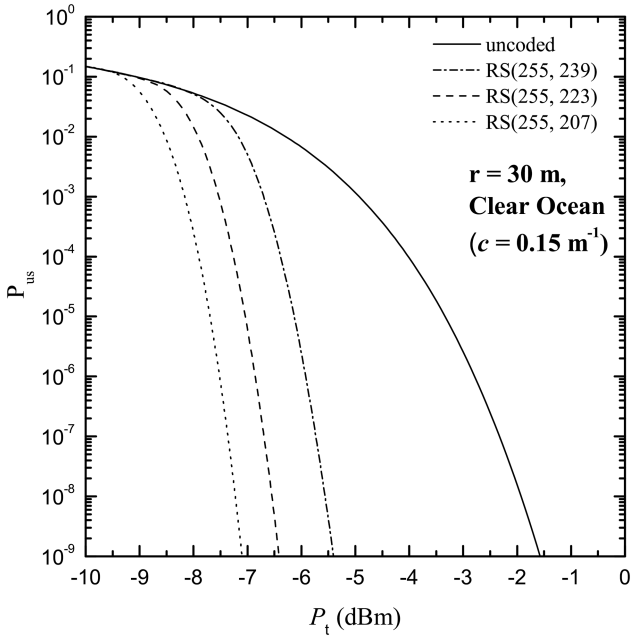

Fig. 6 *Error probability of uncoded and coded SOA-assisted systems as a function of P_t assuming clear ocean ($c = 0.15\ m^{-1}$) for r of 30 m, SOA gain G of 20 dB and various RS encoding schemes*

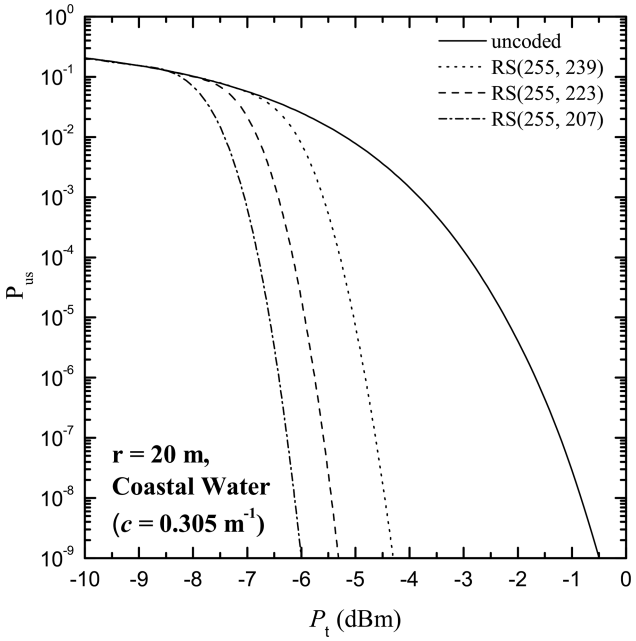

Fig. 7 *Error probability of uncoded and coded SOA-assisted systems as a function of P_t assuming coastal water ($c = 0.305\ m^{-1}$) for r of 20 m, SOA gain G of 20 dB and various RS encoding schemes*

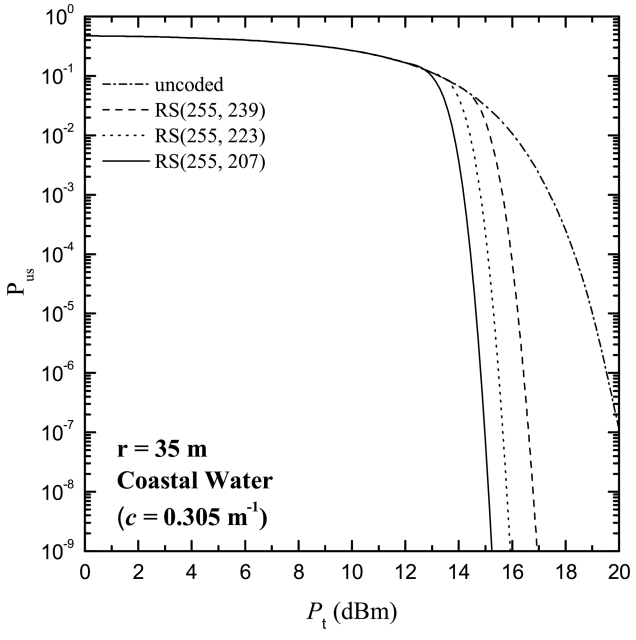

Fig. 8 *Error probability of uncoded and coded SOA-assisted systems as a function of P_t assuming coastal water ($c = 0.305\ m^{-1}$) for r of 35 m, SOA gain G of 20 dB and various RS encoding schemes*

7 References

[1] Gabriel, C., Khalighi, M., Bourennane, S., *et al.*: 'Investigation of suitable modulation techniques for underwater wireless optical communication'. Int. Workshop on Optical Wireless Communications (IWOW), Pisa, October 2012

[2] Cochenour, B.M., Mullen, L.J., Laux, A.E.: 'Characterization of the beam-spread function for underwater optical communications links', *IEEE J. Ocean. Eng.*, 2008, **33**, (4), pp. 513–521

[3] Tang, S., Dong, Y., Zhang, X.: 'On link misalignment for underwater wireless optical communications', *IEEE Commun. Lett.*, 2012, **16**, (10), pp. 1688–1690

[4] Tang, S., Dong, Y., Zhang, X.: 'Impulse response modeling for underwater wireless optical communication links', *IEEE Trans. Commun.*, 2014, **62**, (1), pp. 226–234

[5] Vavoulas, A., Sandalidis, H., Varoutas, D.: 'Underwater optical wireless networks: a k-connectivity analysis', *IEEE J. Ocean. Eng.*, 2014, **39**, (4), pp. 801–809

[6] Jaruwatanadilok, S.: 'Underwater wireless optical communication channel modeling and performance evaluation using vector radiative transfer theory', *IEEE J. Sel. Areas Commun.*, 2008, **26**, pp. 1620–1627

[7] Arnon, S.: 'Underwater optical wireless communication network', *Opt. Eng.*, 2010, **49**, pp. 015001-1–015001-6

[8] Sagias, N., Yiannopoulos, K., Boucouvalas, A.: 'Semiconductor optical amplifiers in negative-exponential fading: regenerators and pre-amplifiers', *IET Optoelectron.*, 2015, **9**, (5), pp. 249–256

[9] Yiannopoulos, K., Sagias, N., Boucouvalas, A.: 'On the performance of semiconductor optical amplifier-assisted outdoor optical wireless links', *IEEE J. Sel. Areas Commun.*, 2015, **33**, (9), pp. 1869–1876

[10] Yiannopoulos, K., Sagias, N., Boucouvalas, A.: 'Fade mitigation based on semiconductor optical amplifiers', *IEEE/OSA J. Lightwave Technol.*, 2013, **31**, (23), pp. 3621–3630

[11] Olsson, N.A.: 'Lightwave systems with optical amplifiers', *J. Lightwave Technol.*, 1989, **7**, (7), pp. 1071–1082

[12] Humblet, P., Azizoglu, M.: 'On the bit error rate of lightwave systems with optical amplifiers', *J. Lightwave Technol.*, 1991, **9**, (11), pp. 1576–1582

[13] Kobayashi, T., Flämmich, M., Jordan, G., *et al.*: 'Blue–green small-signal gain and saturation in a luminescent polymer gain medium', *Appl. Phys. Lett.*, 2006, **89**, (131119), doi: 10.1063/1.2348738

[14] Koda, R., Watanabe, H., Kono, S.: 'Gallium nitride-based semiconductor optical amplifiers', in Garai, S.K. (ED.): '*Some advanced functionalities of optical amplifiers*' (Intech, Rijeka, Croatia, 2015), ch. 2, pp. 27–45

[15] Gabriel, C., Khalighi, M., Bourennane, S., *et al.*: 'Monte-Carlo-based channel characterization for underwater optical communication systems', *IEEE/OSA J. Opt. Commun. Netw. (JOCN)*, 2013, **5**, (1), pp. 1–12

[16] Agrawal, G.P., Olsson, N.A.: 'Self-phase modulation and spectral broadening of optical pulses in semiconductor laser amplifiers', *IEEE J. Quantum Electron.*, 1989, **25**, (1), pp. 2297–2306

[17] Eiselt, M., Pieper, W., Weber, H.G.: 'SLALOM: semiconductor laser amplifier in a loop mirror', *J. Lightwave Technol.*, 1995, **19**, (10), pp. 2099–2112

[18] Agrawal, G.: '*Fiber-optic communication systems*' (Wiley, New York, 2012)

[19] Proakis, J.: '*Digital communications*' (Mc Graw Hill, New York, 2007, 5th edn.)

[20] Arnon, S., Kedar, D.: 'Non line of sight underwater optical wireless communication network', *J. Opt. Soc. Am. A*, 2009, **26**, (3), pp. 530–539

[21] Steel, D.G., Bayvel, L.: '*Encyclopedia of modern optics*' (Elsevier, Oxford, UK, 2004), vol. **1**

[22] Haltrin, V.: 'One-parameter two-term Henyey–Greenstein phase function for light scattering in seawater', *Appl. Opt.*, 2002, **41**, (6), pp. 1022–1028